

Feature Extraction and Classification of Digital Kidney Ultrasound Images: A Hybrid Approach

Sunanda Biradar^{a,*}, Prema T. Akkasaligar^{a,**}, and Sumangala Biradar^{b,***}

^a Department of Computer Science and Engineering (Artificial Intelligence and Machine Learning), BLDEA's V. P. Dr. P.G. Halakatti College of Engineering and Technology, Vijayapur, Karnataka, 586103 India

^b Department of Information Science and Engineering, BLDEA's V. P. Dr. P.G. Halakatti College of Engineering and Technology, Vijayapur, Karnataka, 586103 India

* e-mail: sunanda_biradar@rediffmail.com

** e-mail: premasb@rediffmail.com

*** e-mail: biradarsumangala@gmail.com

Abstract—Ultrasound image is widely used medical imaging modality for the diagnosis of diseases. In this work, a novel hybrid approach for classification of diseased kidney medical ultrasound images is proposed. The segmented images are passed through the stage of feature extraction. Different features, namely, Haralick, shape, wavelet, Tamura, and histogram oriented gradient features are used for classification. The method focuses on recognizing the most dominant feature set that characterizes the texture of a stone, cyst or normal kidney ultrasound image. Extracted features are individually used for classification by three different classifiers namely k -nearest neighborhood, fuzzy k -nearest neighborhood, and support vector machine. The hybrid approach for feature extraction containing the combination of wavelet and shape features shows the optimal classification accuracy. The efficiency of the method is tested with performance parameters such as accuracy, sensitivity, and specificity. The results obtained show the efficiency of the proposed method.

Keywords: kidney stone, polycystic, fuzzy k -nearest neighbor, support vector machine

DOI: 10.1134/S1054661822020043

1. INTRODUCTION

Image processing techniques are widely used in the medical field. Technical up gradation of medical image acquisition devices along with incarnation of advanced computerized algorithms are more specific to the medical image processing, both for diagnostics and treatment plan. Ultrasound imaging is one of the popular imaging methods for acquiring tissue images of the human organ using high-frequency acoustic waves. Reflections of sound waves are recorded as a real-time visual ultrasound image. It is helpful for the examination of human internal organs like kidney, heart, liver, etc.

The kidney is one of the essential organs in the human body, playing a significant role in blood filtration. Every day 0.15 to 0.2 million people undergo dialysis in India. Around 850 million people all over the world are suffering from kidney related diseases [18]. To create awareness, every year on 2nd Thursday of March is celebrated as “World Kidney Day.” Diagnosis and treatment of kidney diseases at the earlier stage is essential. In Section 2, methodology is illustrated.

The details about feature extraction are provided in Section 3. Section 4 explains about the classification process. The results are discussed in Section 5 followed by conclusion in Section 6.

1.1. Overview

Ultrasound imaging is one of the commonly used imaging in medical diagnosis because of its virtues like low cost, harmless, faster acquisition and non-invasive property. However, it has certain disadvantages such as equipment induced noise, noise from its surrounding, the presence of other surrounding tissues and other impacts such as fat, respiration moments, etc. [6]. Therefore, it is challenging to implement computerized algorithms for processing of ultrasound images.

Among different abnormalities of the kidney, stones or renal calculi are the most commonly observed conditions in the human population worldwide. The rate of recurrence of kidney stone is high. Cysts are abnormal sacs containing fluids in the kidney affecting the normal functioning of the organ, leading to the enlargement of the kidney. Polycystic kidney disease is one of the life-threatening diseases. Kidney disease, in turn, can damage the liver, pancreas. Sometimes, the heart and brain can also be severely affected. So, the diagnosis and treatment of

Received October 15, 2021; revised November 1, 2021; accepted December 6, 2021

the kidney disease at the earlier stages is very essential. The increasing numbers of patients with kidney diseases lead to high demand for early detection and prevention of kidney disease. The kidney is imaged to know its morphology (normal or abnormal). The identification of kidney cysts and kidney stones in ultrasound images of the kidney is one of the essential researches concerned with the diagnostic process of kidney disease, its treatment.

1.2. Literature Review

We briefly discuss state of the art on different segmentation, feature extraction and classification algorithms for ultrasound images, available in the literature. In [10], Maulik has shown the use of genetic algorithms for ultrasound image segmentation. In [8], Kumar and Abhishek have experimented on ultrasound kidney images of varying orientations. Kidney organ is rotated, and texture features are extracted to analyze. The angle of rotation is dependent on the input image and is variable for every input. Texture model is used for knowing the inside and outside area of segmenting curve. In [14, 19], an evaluation technique for principal curvature of the multi-scale differential is used. Classification of kidney image is carried out using obtained feature values. In [12], Mendoza et al. have applied the covariance matrix based active shape model. Genetic algorithm is used for adjustment of pose and shape of the kidney organ.

In [16], Subramanya et al. have discussed higher order spline interpolation. Different despeckling methods namely, Gaussian filter, median filter, and Wiener filter are used before classification. Run length texture features and gray level co-occurrence matrix features are used. In [1], classification of non-cystic and cystic kidney medical images by the k -nearest neighbor classifier is implemented. Akkasaligar and Biradar have used the manually segmented image as input. In [13], review of various segmentation algorithms for ultrasound images is available. Noble and Boukerroui have highlighted the different algorithms developed for B-mode ultrasonic images. They have performed a survey of the available methods and mentioned the appropriateness of these methods in different clinical domains. In [11], Meiburger et al. have discussed the segmentation of organs in B-mode ultrasound images. Challenges for segmenting the kidney in ultrasound images like variable shape and size of the organ are elaborated. Classification and segmentation algorithms for 2D and 3D ultrasound kidney images are highlighted. Many existing segmentation methods reveal that the kidney organ is extracted from ultrasound images followed by texture analysis in some

cases. Hence, we propose the extraction of different types of features and further classification using three different classifiers.

In the present paper, the design, and implementation of algorithms using digital image processing techniques for classification of kidney ultrasound images is discussed with the aim to assist the medical experts. Necessary steps involved are as shown below:

- preprocessing and speckle noise removal from input kidney ultrasound image;
- segmentation of normal, cystic or stone portion from preprocessed image;
- finding optimal feature set for normal, stone and cystic kidney ultrasound images;
- classification of the ultrasound images of kidney to find the kidney disease.

2. PROPOSED METHOD

The primary aim of the proposed method is to extract optimal features from segmented kidney ultrasound image and identification of the disease associated with it. The proposed methodology is described in Fig. 1.

2.1. Input Image Set

Digital ultrasound kidney images of various size and alignments are used for the present study. The image database is comprised of clinical image set and images from websites. The clinical database is prepared in consultation with the medical experts of BLDEDU's Sri. B. M. Patil Medical College Hospital and Research Centre, Vijayapur. The Phillips HD11XE ultrasonography machine is used with the curvilinear transducer of 5–7 MHz frequency for the acquisition of images. Web database images are downloaded from public websites such as [<https://openi.nlm.nih.gov>, <https://www.radiology-info.com>, and <https://www.ultrasoundimages.com>]. Both of the datasets contain normal, single-cystic, polycystic, single and multiple kidney stone images.

Sample images of a normal, single cystic, polycystic, single stone and multiple stones of the kidney are depicted in Figs. 2a–2e, respectively.

2.2. Preprocessing and Despeckling

Existence of speckle noise is common in ultrasonic images. Speckle noise leads to poor image quality reducing the analytical capability of ultrasound medical images. So, it is difficult to detect the organ or tissue under consideration because of speckle noise. Hence, despeckling is an essential initial step required before segmentation.

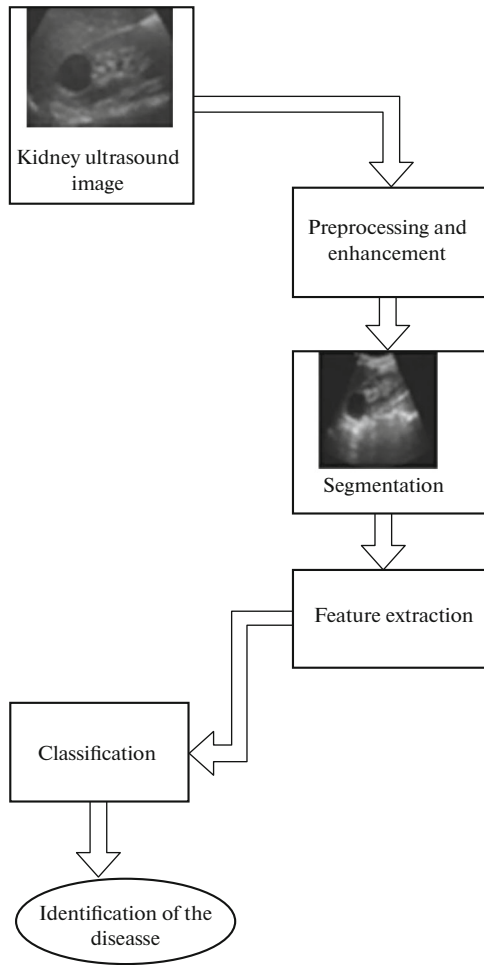


Fig. 1. Block diagram of the proposed methodology.

Speckle noise is of multiplicative type. A logarithmic transform is applied to convert it to additive noise because handling multiplicative noise is tougher. Contourlet transform is more effective in despeckling of ultrasound images [6]. The contourlet transform is carried out in two steps: the Laplacian pyramid (LP) decomposition and applying directional filters bank. LP decomposition is needed to capture the discontinuous points. The directional filter bank is essential for connecting the disconnected points for the absolute organization of points. Hard thresholding is performed. Thresholded image is applied with inverse contourlet transform followed by exponential transform to get the despeckled image. Contrast enhancement is performed by using histogram equalization on the despeckled image to get a better quality image.

2.3. Segmentation

Segmentation is the process of dividing the image into homogeneous regions. It helps in detecting the required region of interest (ROI) in an image.

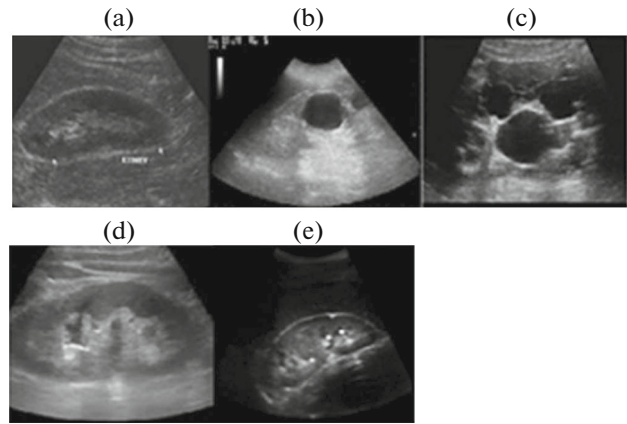


Fig. 2. Sample kidney ultrasound images: (a) normal kidney ultrasound image, (b) single cystic kidney ultrasound image, (c) polycystic kidney ultrasound image, (d) single stone kidney ultrasound image, and (e) multiple stone kidney ultrasound image.

Despeckled kidney ultrasound images are segmented to obtain ROI of cysts or stones. Automatic segmentation of ROI can be performed without user intervention. The level set method is found to be the efficient, automatic and more accurate segmentation of single and multiple cysts as well as stones [2, 3].

The structural information obtained during the segmentation provides an essential visual aid for image-guided surgery.

3. EXTRACTION OF FEATURES

Feature extraction converts the image to a vector of features. Features are commonly made of information such as shape, color, texture, etc. Seven sets of features suitable for kidney ultrasound images for classification of the input image as cystic and stone image are discussed in this section.

3.1. Haralick Features

Gray level co-occurrence matrix (GLCM) based extraction of features for classification of different types of images was initially explained by Haralick et al. [5]. These features are widely used in image analysis, particularly, in the medical image processing. The working of Haralick features extraction is done in two major steps. Computation of GLCM is the initial step, followed by extraction of texture features on the obtained GLCM. It works on the spatial arrangement of pixels. The frequency of occurrence of specific pixel value pairs in a specific spatial relationship is computed in GLCM. The GLCM can be applied on a square matrix in which two pixels in the neighborhood are separated by a mentioned distance “d” at an orientation of “o.” It represents the comparative frequency distribution of gray levels and explains how frequently

a particular gray level will appear in a specific spatial arrangement. Various GLCM texture features like energy homogeneity, contrast and correlation are calculated for classification of segmented kidney ultrasound images. The details of the process of feature extraction using GLCM are shown in Algorithm 1.

Algorithm 1. Haralick texture features extraction.

Input. Segmented kidney ultrasound image (P).

Output. A vector of sixteen Haralick texture features.

Start

Step 1. Read the input image P .

Step 2. Obtain GLCM matrices in four directions i.e., 0° , 45° , 90° , 135° and a distance of 1 for the read input image.

Step 3. Compute the features namely energy, homogeneity, contrast and correlation by using Eqs. (1)–(4), respectively for all the four matrices.

$$\mu = \sum_{x,y} xP(x,y), \quad (1)$$

$$\sigma = \sum_{x,y} (x - \mu)^2 P(x,y), \quad (2)$$

$$\text{Contrast} = \sum_{xy} |x - y|^2 P(x,y), \quad (3)$$

$$\text{Correlation} = \sum_{xy} \frac{(x - \mu)(y - \mu)P(x,y)}{\sigma^2}, \quad (4)$$

where μ is weighted avg. of pixel and σ is weighted variance of pixel.

Step 4. Store the 16 calculated feature values in a vector.

Stop.

3.2. Shape Features

Images are represented by different forms that explain about the object shape and size. The kidney cysts and stones are oval shaped structures, resembling the elliptical shape. Hence, the parameters describing the ellipse shape can accurately identify/categorize the stone and cysts. Different shape feature descriptors namely, area, perimeter, diameter, orientation, eccentricity, major and minor axis length are used effectively for image analysis and classification.

Area. It is the total number of pixels covering the segmented kidney stone or cystic region and is calculated as in Eq. (5)

$$\text{Area} = \sum_{i=1}^n \sum_{j=1}^m P(i,j). \quad (5)$$

Major axis length. It is obtained by the diameter of the largest circle circumscribed by the segmented stone or cystic region and is shown as in Eq. (6)

$$\text{Maj_axis} = \sqrt{(x_1 - x_2)^2 + (y_1 - y_2)^2}. \quad (6)$$

Minor axis length. It is obtained by the diameter of the smallest circle circumscribed by the segmented stone or cystic region and is shown as in Eq. (7)

$$\text{Min_axis} = \sqrt{(x_2 - x_1)^2 + (y_2 - y_1)^2}. \quad (7)$$

In Eqs. (6) and (7), (x_1, y_1) and (x_2, y_2) are the end points of the axes.

Eccentricity. Eccentricity is defined by the ratio between major axis length and minor axis length. It is expressed as in Eq. (8)

$$\text{Eccentricity} = \frac{\text{Major_axis}}{\text{Minor_axis}}. \quad (8)$$

Orientation. It is a scalar value that represents the angle between the horizontal axis and the major axis of the diseased kidney region.

3.3. Wavelet Features

Wavelet considers both time and frequency domain knowledge of image. Wavelet transform can be effectively used in image processing for various applications such as compression, image analysis, speckle noise removal of medical images [4], etc. In wavelet decomposition a 2D image is decomposed into four frequency sub-bands, namely, the LL, HL, LH, and HH bands. H symbolizes high pass filter and L indicates low pass filter. LL is obtained by applying a low pass filter for both horizontal and vertical directions. LH is obtained by applying a low pass filter for horizontal and high pass filter for vertical directions. HL is obtained by applying a high pass filter for horizontal and low pass filter for vertical directions. HH is obtained by applying a high pass filter for both horizontal and high p vertical directions. In higher decomposition levels, LL subband alone is taken for further subdivision because, it represents the approximate coefficients. Energy feature obtained at horizontal, vertical, and diagonal subbands are considered as features for classification of diseased kidney ultrasound images.

Various wavelet families are available like Daubechies, discrete symlets, biorthogonal, reverse biorthogonal, Meyer, and coiflets.

3.4. Tamura Features

Tamura features work on the visual perception of humans. They contribute potentially for representation of image. Tamura features work on homogeneous nature of texture [17]. Coarseness is related to the distance of spatial differences of gray levels. It is the measure of the texels forming the texture. The computed features take into account of variation between the average signals for the non-overlapping windows of various sizes.

Coarseness. It is the measure significant spatial variation of grey levels. In other words, it refers to the size of the significant pixels framing the texture.

Contrast. It is a measure of grey levels distribution in the image and the extent to which the gray levels are biased towards black or white.

Direction. Direction is a measurement of the frequency distributions of oriented edges versus their directional angle.

3.5. Histogram of Oriented Gradient (HOG) Features

HOG feature set is used for object detection in image classification. It considers number of occurrences of gradient orientation in region of interest (ROI). HOG feature extraction is explained with the following Algorithm 2.

Algorithm 2: HOG features extraction

Input. Segmented kidney ultrasound image (P).

Output. A vector of HOG texture features.

Start

Step 1. Read the input image P.

Step 2. Split the image into smaller connected components of size 5×5 called cells.

Step 3. For each cell calculate HOG directions for the pixels of the cell.

Step 4. Discretize every cell to 9 angular bins as per the gradient directions 0° to 160° at a difference of 20° .

Step 5. Blocks of adjacent cells is to be framed on the basis of histograms normalization.

Step 6. The block histograms should be stored as feature descriptors.

Stop.

Different feature sets obtained are used for classification purpose.

4. CLASSIFICATION

Several classification methods are used in the field of pattern recognition. Classifiers are widely used in various fields such as statistics, artificial intelligence, medicine, etc. Parametric types of classifiers require perfect training for acquiring priori knowledge. They are suitable for classification problems having a larger dataset. In several cases, it is not easy to find larger priori information. In such cases, non-parametric classifiers are more suitable. The proposed system uses n-fold classifiers.

4.1. *k*-Nearest Neighbors (*k*-NN) Classifier

The *k*-nearest neighbors algorithm is a non parametric classification algorithm. It classifies the input pattern on the basis of class labels that most of the “*k*” nearest neighbors from the training data possesses. The algorithm has several benefits like.

- Simpler to design and implement;
- faster and suitable for smaller training samples;
- no priori knowledge about the training is needed;
- better performance.

k-NN classifier needs a user specified value for constant *k* and a feature vector without label for testing. The feature vector obtained for a sample image is classified to a class label based on the *k* training sets nearer and frequent among training set. The *k*-NN is not defined by explicit training. However, the complete training set is required during the classification stage unlike other supervised classifier. Thus, the larger amount of time consumed for training is reduced completely.

For the *n* classes, $c_1, c_2, c_3, \dots, c_n$, and the unknown sample *T*, *k*-NN judge that the majority vote for *k* nearest neighbors belongingness to one class using Euclidean distance. The decision function [9] is as in Eq. (9). We have used a classifier with the class labels as normal class, stone and cystic kidney ultrasound image.

$$Di(T) = \max(ki) \quad (9)$$

for $i = 1, 2, \dots, n$.

4.2. Fuzzy *k*-Nearest Neighbors (*k*-NN) Classifier

In case of fuzzy *k*-NN, the decision of class is made by using the relation between distance and similarity. The distance between *T* and C_i can be shown as in Eq. (10)

$$\text{dist}(T, C_i) = 1 - \text{sim}(T, C_i), \quad (10)$$

where $\text{sim}(T, C_i)$ denotes the similarity between training image set and testing image. *k*-Nearest neighbors’ known samples $\{T_i, 1, 2, \dots, k\}$ of the classifying sample *T*, are computed as the members of a sample *T* to each class as specified [9] in Eq. (11)

$$\mu_j(T) = \frac{\sum_{i=1}^k \mu_j(T_i) \text{sim}(T, T_i) \frac{1}{(1 - \text{sim}(T, T_i))^{2/(b-1)}}}{\sum_{i=1}^k \frac{1}{(1 - \text{sim}(T, T_i))^{2/(b-1)}}} \quad (11)$$

If sample *T* belongs to *j* class then the value is 1, otherwise 0. From the equation, it is seen that the membership is decided based on the distance of every neighbor to the testing sample to weigh its effect. The variable *b* is adjusts the degree of a distance weight. In this method, we take the value of *b* as 2 always. Optimal value of *b* is between 1.5 and 2.5 as specified in [9].

4.3. Support Vector Machine (SVM) Classifier

SVM uses explicit training and shows good performance even with unknown data sample classification. SVM is applied to a wide variety application including classification of medical images [16]. It has been

Table 1. Haralick features

Feature	Value	Feature	Value
Energy for 0°	0.695702	Energy for 90°	0.697924
Homogeneity for 0°	0.980689	Homogeneity for 90°	0.986056
Contrast for 0°	1.051347	Contrast for 90°	0.748175
Correlation for 0°	0.924081	Correlation for 90°	0.946684
Energy for 45°	0.693380	Energy for 135°	0.694239
Homogeneity for 45°	0.970700	Homogeneity for 135°	0.971574
Contrast for 45°	1.610263	Contrast for 135°	1.565140
Correlation for 45°	0.880155	Correlation for 135°	0.883513

Table 2. Shape features

Feature	Value	Feature	Value
Area	2158.0000	Extent	0.179654
Convex area	12012.000	Filled area	12012.00
Eccentricity	0.571351	Orientation	86.458719
Equi-diameter	52.418040	Perimeter	432.79600
Major axis length	184.68572	Solidity	0.179654
Minor axis length	151.57263		

found to perform superior than any other classifier. The SVM kernel function is a key function used for inherent mapping of the kidney image to a high-dimensional feature set. The higher dimensional data representation provides better separation compared to linear representation. Two types of kernel functions usually used are polynomial and radial basis function (RBF) kernel. We have used RBF kernel function for classification.

5. RESULTS AND DISCUSSION

Implementation and results obtained for the proposed algorithms are discussed in this section.

5.1. Experimental Setup

The implementation of the proposed algorithm is carried out using MATLAB R2018b. Kidney medical ultrasound images of different sizes and orientations are used for experimentation. The input image dataset of 185 US images is taken from two resources and labeled as D1 and D2. D1 set contains USG kidney images collected from BLDEDU's Shri. B.M. Patil Medical College Hospital and Research Centre, Vijayapur. The images in D2 set are obtained

from web resources (<https://openi.nlm.nih.gov>, <https://www.sonoworld.com>, and <https://www.ultrasoundimages.com>). The input dataset 37 normal kidney images, 39 single-cystic, 35 polycystic, 38 single-stone, and 36 multiple-stones images altogether.

Ground truth images (manually marked) are collected from medical experts. Inkscape image editor is used for constructing the ground truth image database.

Speckle noise removal is carried out by using contourlet transform. Contrast of noiseless images is enhanced through histogram equalization. Automatic level set segmentation is applied to get required region of interest (ROI) containing diseased region of the input image such as cystic portion or region containing stone region. We mainly discuss about extraction of features from the segmented images using different feature set. The extracted features are used for classification of normal and diseased kidney ultrasound images using different classifiers.

5.2. Feature Extraction

Various features are extracted from segmented ultrasound kidney image. Haralick features, and shape

Table 3. Wavelet features

Subband and Wavelet family	Energy features at level 1 (6)	Energy features at level 2 (6)	Energy features at level 3 (6)
Horizontal, db3	25.45129	3.957883	-5.82316
Vertical, db3	0.002469	59.55016	7.160658
Diagonal, db3	0.980392	0.002595	0.127515
Horizontal, bior3.5	0.001841	0.709804	8.814809
Vertical, bior3.5	-0.34996	0.394031	-2.64764
Diagonal, bior3.5	3.984314	4.227144	4.117647

features extracted from a sample image are shown in Tables 1 and 2, respectively. Table 1 shows the total of 16 features calculated on GLCM matrix obtained in 0°, 45°, 90°, and 135°. For each of the GLCM, four features namely, energy, homogeneity, contrast, and correlation are computed.

Table 2 shows the geometrical shape features obtained for a sample diseased kidney ultrasound image. Shape features are efficiently contributing in separation of cystic kidney disease from kidney stone because of the prominent variation in shape and size of the cysts and stones in kidney ultrasound images.

We have experimented with various wavelet families such as Daubechies, Haar, symlets, and biorthogonal filters and their combinations. Discrete wavelet transform with different levels of decompositions is also tested. It is found that wavelet energy feature extracted using Daubechies and biorthogonal filters are more suitable. Decomposition upto level 3 is considered as optimal empirically as specified in [4]. We get totally 9 features for one family of wavelet filters at level 3. Three features at first level (vertical, horizontal, and diagonal sub-bands), three at level 2 and three features at level 3 are considered. Totally, 18 features are obtained, i.e., nine features for each wavelet family. Features obtained for a sample image are shown in Table 3.

Tables 4 and 5 show the Tamura features, and HOG features extracted for a sample image respectively. The HOG features obtained are showing the sample values obtained for nine angular bins obtained in the gradient angles of 0°, 20°, 40°, 60°, 80°, 100°, 120°, 140°, and 160° respectively considering the range from 0° to 180° with a difference of 20°. Either 0° or 180° is included as they result into similar gradient direction.

5.3. Classification and Performance Evaluation

Different classifiers like *k*-NN, fuzzy *k*-NN, and SVM are used on different features extracted for classification of diseased kidney ultrasound images into normal class, kidney stone class and cystic disease class. *k* Value of 3 is found as optimal in case of *k*-NN

and fuzzy *k*-NN. The 5-fold classification is performed and average accuracy is calculated for all the three classifiers. For all the three classifiers the training and testing sets are selected using a 5-fold method. In 5-fold method, the whole dataset is divided into 5 parts randomly, 3 parts (60% of the total 185 images taken randomly) are used for training and remaining images are used for testing. In each pass, 111 images are selected for training and 74 images for testing. Totally five passes are carried out and the average values of performance metrics of all the five iterations are taken into account. The evaluation of the performance of the proposed classification algorithms are carried out by using the parameters such as accuracy, sensitivity and specificity. Average classification accuracy for individual feature sets using *k*-NN, fuzzy *k*-NN, and

Table 4. Tamura features

Feature	Value
Coarseness	16.587912
Contrast	69.461463
Direction	0.811167

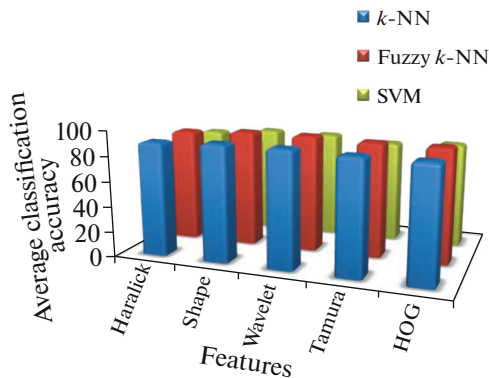
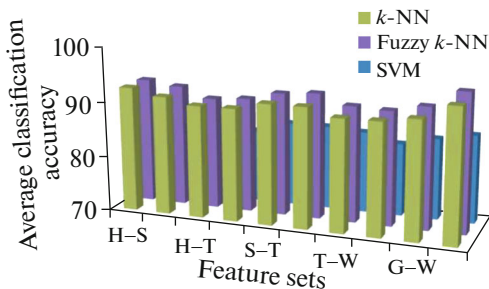
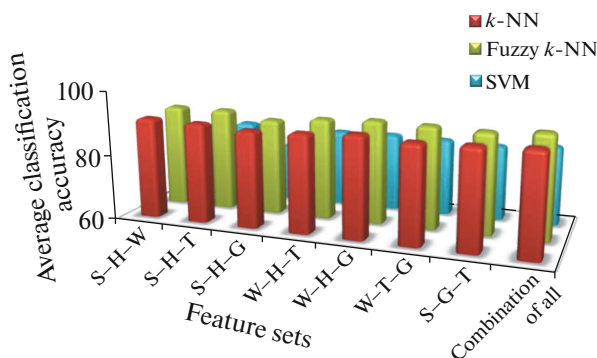
Table 5. HOG features

Feature descriptor	0°	20°	40°	60°	80°	100°	120°	140°	160°
Feature descriptor at 0°	0.0723	0.0805	0.2025	0.0140					
Feature descriptor at 20°	0.0086	0.3264	0.3264	0.3264					
Feature descriptor at 40°	0.0072	0.0068	0.0600	0.1489					
Feature descriptor at 60°	0.0169	0.0105	0.0136	0.1339					
Feature descriptor at 80°	0.0619	0.0130	0.0086	0.0140					
Feature descriptor at 100°	0.0160	0.0947	0.3264	0.0123					
Feature descriptor at 120°	0.3264	0.1506	0.3264	0.0320					
Feature descriptor at 140°	0.0028	0.0041	0.0286	0.5693					
Feature descriptor at 160°	0.1818	0.7130	0.1106	0.3482					

Table 6. Confusion matrix for hybrid model using fuzzy k -NN

	Cystic kidney	Kidney stone	Normal kidney
Cystic kidney	45	0	0
Kidney stone	1	22	1
Normal kidney	1	0	25

SVM are shown in Fig. 3. Wavelet feature set obtained at level 1, level 2, and level 3 are classified using the three classifiers. Figure 3 shows that shape and wavelet

**Fig. 3.** Average classification accuracy for different classifiers using individual feature sets.**Fig. 4.** Average classification accuracy for different classifiers using various combination of two feature sets.**Fig. 5.** Average classification accuracy for different classifiers using various combination of three and all feature sets.

features result in comparatively better classification accuracy.

The model is tested for classification accuracy at different wavelet levels. Decomposition level 3 is found as optimal level. We have also tested the combination of two and three feature set as shown in Figs. 4 and 5 respectively. Labels H, S, W, T, and O indicate Haralick, shape, wavelet, Tamura, and HOG feature sets respectively. Figure 4 shows the plot of average classification accuracy obtained by combining two different feature sets of all possibilities such as shape–Haralick (S–H), wavelet–Tamura (W–T), etc. Among all these combinations, shape–wavelet (S–W) is the optimal feature set as shown in the last column of the graph in Fig. 4.

We have explored the hybrid approach for selection of optimal feature sets for classification of diseased medical ultrasound images of kidney. The combined feature set includes shape and wavelet features. It is observed that the fuzzy k -NN classifier performs better compared to k -NN and SVM for the proposed method. Table 6 shows the confusion matrix for the average values obtained on shape and wavelet hybrid feature model using five-fold fuzzy k -NN classifier.

The proposed hybrid model containing wavelet and shape features, using fuzzy k -NN classifies the input normal, cystic and kidney stone images with an accuracy of 96.68%. However, it classifies cystic images 100% accurately, as cysts are prominently visible sacs found in kidney ultrasound images of cystic disease.

The proposed method can be compared with the method in [7], where a classification accuracy of 89 and 84% using k -NN and SVM classifiers is achieved in identification of kidney stones in ultrasound images. In [8], laboratory blood test parameters are used for identification of kidney stones using artificial neural networks, and an accuracy of 92% is achieved. The proposed method can be compared with our earlier developed method in [4], where an entire image is used for classification purpose. The classification accuracy of 96.68%, in the proposed method is obtained by fuzzy k -NN classifier with hybrid feature set of shape and wavelets features is found to be better than 93.75% obtained in [4]. The proposed method is also able to detect cystic kidney disease along with renal calculus and normal kidney images effectively.

From the experimental results, it is observed that the supervised classifiers such as SVM are not suitable for the smaller training sets. Another added advantage of non-parametric classifiers like k -NN and fuzzy k -NN is substantial reduction in training time.

6. CONCLUSIONS

In this paper, a hybrid approach, combining shape based and wavelet features set for classification is proposed. Kidney medical ultrasound image read as input is classified as normal, cystic or stone type. Prepro-

cessed and segmented ultrasound images of kidney using level set method are used as input by feature extraction module. Individual feature sets like Haralick, shape, wavelets, Tamura, and histogram oriented gradient features are extracted. Extracted features are individually classified by three different classifiers namely k -NN, fuzzy k -NN, and SVM. Accuracy rate of 96.68% is achieved using fuzzy k -NN with combined features set. The performance of the proposed method is also measured using sensitivity and specificity. The values of sensitivity and specificity for hybrid features using fuzzy k -NN classifier are 0.984 and 0.958, respectively. The proposed algorithm can be used for clinical analysis of kidney medical ultrasound images by the medical experts.

FUNDING

The work is financially supported by Vision Group of Science and Technology (VGST), Government of Karnataka under RGS/F scheme (GRD no. 729/2017-18).

ACKNOWLEDGMENTS

Authors would like to thank Dr. Bhushita B. Lakhkar, Radiologist, BLDEDU's Shri. B.M. Patil Medical College Hospital and Research Centre, Vijayapur for providing USG image set of kidney. Authors are also thankful to Dr. Vinay Kunderagi, Nephrologist, BLDEDU's Shri. B.M. Patil Medical College Hospital and Research Centre, Vijayapur for rendering manual segmentation of images.

COMPLIANCE WITH ETHICAL STANDARDS

This article is a completely original work of its authors; it has not been published before and will not be sent to other publications until the *PRIA* Editorial Board decides not to accept it for publication.

Conflict of Interest

The authors declare that they have no conflicts of interest.

REFERENCES

1. Prema T. Akkasaligar and S. Biradar, "Classification of medical ultrasound images of kidney," *Int. J. Comput. Appl., Special Issue on ICICT*, 32–36 (2014).
2. Prema T. Akkasaligar and S. Biradar, "Segmentation of kidney stones in medical ultrasound images," in *Recent Trends in Image Processing and Pattern Recognition. RTIP2R 2018*, Ed. by K. Santosh and R. Hegardi, Communications in Computer and Information Science, vol. 1036 (Springer, Singapore, 2019), pp. 200–208. https://doi.org/10.1007/978-981-13-9184-2_18
3. Prema T. Akkasaligar and Sunanda Biradar, "Automatic segmentation and analysis of renal calculi in medical ultrasound images," *Pattern Recognit. Image Anal.* **30**, 748–756 (2020). <https://doi.org/10.1134/S1054661820040021>
4. Prema T. Akkasaligar and Sunanda Biradar, "Diagnosis of renal calculus disease in medical ultrasound images," in *IEEE Int. Conf. on Computational Intelligence and Computing Research (ICIC), Chennai, India, 2016* (IEEE, 2016), pp. 1–5. <https://doi.org/10.1109/ICIC.2016.7919642>
5. R. M. Haralick, K. Shanmugam, and I. Dinstein, "Textural features for image classification," *IEEE Trans. Syst., Man Cybern.* **3**, 610–621 (1973). <https://doi.org/10.1109/TSMC.1973.4309314>
6. P. S. Hiremath, Prema T. Akkasaligar, and S. Badiger, "Speckle reducing contourlet transform for medical ultrasound images," *Int. J. Comput. Inf. Eng.* **5**, 932–939 (2011). <https://doi.org/10.5281/zenodo.1062772>
7. V. Jyoti, M. Nath, P. Tripathi, and K. K. Saini, "Analysis and identification of kidney stone using k th nearest neighbour (k NN) and support vector machine (SVM) classification techniques," *Pattern Recognit. Image Anal.* **27**, 574–580 (2017). <https://doi.org/10.1134/S1054661817030294>
8. K. Kumar and Abhishek, "Artificial neural networks for diagnosis of kidney stones disease," *Int. J. Inf. Technol. Comput. Sci.* **7**, 20–25 (2012). <https://doi.org/10.5815/ijitcs.2012.07.03>
9. S. Manish, "Fuzzy-rough nearest neighbor algorithms in classification," *Fuzzy Sets Syst.* **158**, 2134–2152 (2017). <https://doi.org/10.1016/j.fss.2007.04.023>
10. U. Maulik, "Medical image segmentation using genetic algorithms," *IEEE Trans. Inf. Technol. Biomed.* **13**, 166–173 (2009). <https://doi.org/10.1109/TITB.2008.2007301>
11. K. M. Meiburger, U. R. Acharya, and F. Molinari, "Automated localization and segmentation techniques for B-mode ultrasound images: A review," *Comput. Biol. Med.* **92**, 210–235 (2018). <https://doi.org/10.1016/j.compbiomed.2017.11.018>
12. C. S. Mendoza, X. Kang, N. Safdar, E. Myers, C.A. Peters, and M. G. Linguraru, "Kidney segmentation in ultrasound via genetic initialization and active shape models with rotation correction," in *IEEE 10th Int. Symp. on Biomedical Imaging, San Francisco, 2013* (IEEE, 2013), pp. 69–72. <https://doi.org/10.1109/ISBI.2013.6556414>
13. J. A. Noble and D. Boukerroui, "Ultrasound image segmentation: A survey," *IEEE Trans. Med. Imaging* **25**, 987–1010 (2006). <https://doi.org/10.1109/TMI.2006.877092>
14. K. B. Raja, M. Madheswaran, and K. Thyagarajah, "Quantitative and qualitative evaluation of us kidney images for disorder classification using multi-scale differential features," *ICGST-BIME J.* **7** (1), 1–8 (2000).
15. K. B. Raja, M. Madheswaran, and K. Thyagarajah, "A general segmentation scheme for contouring kidney region in ultrasound kidney images using improved higher order spline interpolation," *Int. J. Biol. Life Sci.* **2** (2), 81–88 (2007). <https://doi.org/10.5281/zenodo.1081870>

16. M. B. Subramanya, V. Kumar, S. Mukherjee, and M. Saini, "SVM-based CAC System for B-mode kidney ultrasound images," *J. Digital Imaging* **28**, 449–458 (2015).
<https://doi.org/10.1007/s10278-014-9754-4>
17. H. Tamura, S. Mori, and T. Yamawaki, "Textural features corresponding to visual perception," *IEEE Trans. Syst., Man, Cybern.* **8**, 460–473 (1978).
<https://doi.org/10.1109/TSMC.1978.4309999>
18. Test your kidneys without fail. Vijayavani. <http://epa-pervijayavani.in/index.php?dated=2019-03-15>. Cited March 16, 2019.
19. J. Xie, Y. Jiang, and H. Tsui, "Segmentation of kidney from ultrasound images based on texture and shape priors," *IEEE Trans. Med. Imaging* **24**, 45–57 (2005).
<https://doi.org/10.1109/TMI.2004.837792>



Dr. Sunanda Biradar is working as Assistant Professor in department of Computer Science and Engineering of College of Engineering and Technology, Vijayapur, Karnataka, India. She has completed her Bachelor of Engineering from Visvesvaraya Technological University Belagavi, Karnataka, India in the year 2002. M.Tech. (CSE) from Visvesvaraya Technological University, Belagavi, Karnataka, India in 2009 and PhD from Visvesvaraya Tech-

nological University, Belagavi, Karnataka, India in 2021. Her areas of interest are medical image processing and pattern recognition. She has more than 15 research publications in reputed and peer reviewed international journals, conference proceedings, and book chapters. She has also received research fund from Vision Group of Science and Technology (VGST), KBITS, Govt. of Karnataka and KSCST, Karnataka.



Prema T. Akkasaligar has completed her Bachelor of Engineering from Karnataka University Dharwad in the year 1995, ME (CSE) from Gulbarga University, Gulbarga in 1999 and PhD from Gulbarga University, Gulbarga in 2013. Currently, she is working as Professor in the Department of Computer Science and Engineering of BLDEA's V.P. Dr. P.G.H. College of Engineering and Technology, Vijayapur, Karnataka, India. She has more than

35 research publications in reputed and peer reviewed international journals, conference proceedings, and book chapters. She is life member of Computer Society of India (CSI), The Institution of Engineers, India (IEI), Life Member of Indian Society for Technical Education (ISTE), and International Association of Computer Science and Information Technology (IACSIT), Singapore. She has also received research fund from KBITS, Govt. of Karnataka and FOSS scheme of VTU Belagavi, Karnataka. Her areas of interest are medical image processing and computer vision.



Mrs. Sumangala Biradar is working as Assistant Professor in department of Information Science and Engineering of College of Engineering and Technology, Vijayapur, Karnataka, India. She has completed her Bachelor of Engineering from Visvesvaraya Technological University Belagavi, Karnataka, India in the year 2002. M.Tech. (CSE) from Visvesvaraya Technological University, Belagavi, Karnataka, India in 2011 and PhD (pursuing). From Visvesvaraya Technological

University, Belagavi, Karnataka, India. Her areas of interest are machine learning, information security, and cryptography. She has published papers in reputed and peer reviewed international journals and conference proceedings. She has also received research fund from Vision Group of Science and Technology (VGST), Karnataka.